Online Monitoring of Copolymerization Involving Comonomers of Similar Spectral Characteristics

Alina M. Alb, Pascal Enohnyaket, Michael F. Drenski, Aaron Head, Alex W. Reed, and Wayne F. Reed*

Physics Department, Tulane University, New Orleans, Louisiana 70118

Received April 9, 2006; Revised Manuscript Received June 14, 2006

ABSTRACT: Automatic continuous online monitoring of polymerization reactions (ACOMP) was applied to free radical copolymerization of acrylic comonomers, whose spectral characteristics are very similar. Determination of the instantaneous concentration of each comonomer during the reaction was made possible by incorporating a full spectrum UV spectrophotometer into the detector train. The working assumption was that a UV spectrum at any instant during conversion is a linear combination of the normalized basis spectra of the comonomers and the copolymer, and that the unknown comonomer concentrations can be found by minimizing the error between measured and computed spectra over many wavelengths, even when spectral differences are small at any given wavelength. Here, the copolymerization of butyl acrylate (BA) and methyl methacrylate (MMA) was monitored under different starting composition ratios. Continuous conversion kinetics, composition drift, and average composition distribution are all found from the data, in addition to the evolution of weight-average intrinsic viscosity and molar mass M_w. Reactivity ratios, $r_{mma} = 0.40 \pm 0.05$ and $r_{ba} = 2.58 \pm 0.1$, are close to the averages found from a literature survey over a wide range of conditions. Comonomer conversion results were independently cross-checked by GPC. Increasing the content of BA in the copolymer was found to increase M_w, while also leading to a significant increase in chain stiffness. This work sets the stage for extension to copolymerization of three and more comonomers.

Introduction

Copolymers can provide novel properties by synergizing characteristics of their constituent comonomers.[1−3] Block and statistical copolymers show different interactions with each other and other polymers, including micellization, and complex phase and surface behavior.[4−11] Important copolymer characteristics include the bivariate distribution in composition and molecular mass,[12−14] reactivity ratios, and sequence length distributions.[15−17]

Differential conversion rates for comonomers causes composition drift during copolymerization and a resulting composition distribution in the final product. Molar mass and intrinsic viscosity may also evolve during such reactions. These various distributions are expected to affect the macroscopic properties of the copolymers.

The composition and molar mass bivariate distribution is a way of characterizing these central characteristics of a copolymer product. *Post-polymerization* analysis for determining the bivariate distribution currently relies on cross-fractionation and other coupled techniques on copolymeric end products. These include calorimetry and densimetry,[18] liquid chromatography,[19] temperature rising elution fractionation,[20−23] crystallization analysis fractionation,[24] and techniques involving multidetector SEC alone,[25,26] SEC/NMR,[27] SEC/MALDI,[28] and SEC/thin-layer chromatography.[29,30] Chromatographic techniques for composition analysis were recently reviewed.[31] Temperature gradient interaction chromatography is a promising development for composition analysis, but it requires long detailed studies of solvent mixtures and temperature gradients to be effective.[32]

There has been a growing amount of work using near-infrared (NIR) and Raman spectroscopy to *monitor* homo- and copolymerization reactions in situ.[33−39] In principle, these techniques are very convenient because they require no sample extraction or preparation.

Automatic continuous online monitoring of polymerization reactions (ACOMP) was introduced in 1998,[40] and provides a means of following the evolution of the average composition and molar mass distributions during the reaction. It is a nonchromatographic technique that requires the continuous withdrawal of a small sample stream from the reactor, which is diluted to the degree that measurements made on the flowing sample are dominated by single particle properties and not by polymer interactions. Typically, combining multiangle light scattering, ultraviolet absorption, viscometry, and differential refractometry allows the determination of monomer conversion and measures of polymer molecular mass. It has been successfully applied to free radical and controlled free radical gradient copolymerization,[41,42]

It is interesting to compare ACOMP with in situ methods such as NIR and Raman. While ACOMP gives the comonomer conversions, which those techniques also do, ACOMP additionally monitors the evolution of M_w and $[\eta]_w$, average polymer properties of critical importance in the ultimate characterization and utilization of the polymers.

An advantage of Raman and NIR compared to ACOMP is that probes for the former can often be put inside the reactor, avoiding ACOMP's complex withdrawal, dilution, and conditioning steps. The in situ probes also eliminate the delay times inherent to ACOMP. On the other hand, whether a probe is inserted into a reactor or a tube for withdrawal is inserted for ACOMP, access into the reactor is required in either case, and hence all techniques are "invasive" to this degree. Furthermore, probes inside of reactors can easily foul and lead to erroneous data. Working at high concentrations in the reactor often requires that empirical models and calibrations be used to interpret data.[43] In fact, calibration difficulties with Raman are well-known, and whole articles are devoted to them.[44] In contrast, the "front-end" (extraction, dilution, and conditioning, such as filtration, debubbling, phase inversion, etc.) of ACOMP is a flexible

10.1021/ma060800f CCC: $33.50
Published on Web 08/01/2006

platform and specifically designed to deal with the conversion of real, often "dirty" and nonideal reactor contents into a highly conditioned, dilute, and continuous sample stream on which absolute, model-independent measurements can be made.

The goal of this work is to extend ACOMP to the case where copolymerization of comonomers of only slightly different spectral characteristics are used.

Materials and Methods

Compounds and Polymerization Reactions. MMA and BA were supplied by Aldrich and used as received. Butyl acetate, the reactor and ACOMP dilution solvent, was also from Aldrich, as well as the initiator, AIBN. Reactions were carried out with a total of 30% by mass comonomers in butyl acetate, in a total reaction volume mass of 250 mL. Reactions were carried out in a thermostated three neck reactor under and N_2 blanket at 66 °C.

ACOMP System. The ACOMP system withdrew reactor liquid at 0.1 mL/min, with a total detector flow rate of 2.0 mL/min (i.e., 20/1 dilution), yielding 0.014 g/mL of total monomer in the detector train. A simple two-pump front end was used in the configuration first introduced by Chauvin et al.[45] A Shimadzu HPLC pump and a Kratos HPLC pump were used in tandem. The concentration of comonomers was kept correspondingly low (30% by mass) in the reactor to avoid the problems of high viscosity that can be overcome with the full five-pump, dual mixing chamber instrumentation later introduced by the authors (Mignard et al.[41]). ACOMP has frequently been used to measure bulk polymerization, and the current copolymerization reactions could also be carried out in bulk. It is also noted that ACOMP has been used to monitor reactions in emulsions and inverse emulsions.[46]

The ACOMP detectors included a Shimadzu PDA-20 photodiode array for full spectrum UV absorbance, a Brookhaven Instruments Corporation BI-MwA 7 angle light scattering instrument, a home-built single capillary viscometer,[47] a dual wavelength Shimadzu UV spectrophotometer (as a redundant cross-check on the PDA-20), and a Waters 410 RI. The delay time between withdrawal from the reactor and detection was approximately 180 s.

Automatic Continuous Mixing (ACM). ACM is a convenient means of characterizing second virial coefficient A_2 and cross-checking ACOMP values for M_w and $[\eta]_w$.[48] ACM measurements on end products were made using a Shimadzu gradient mixing pump adapted to the ACOMP detector train.

Gel Permeation Chromatography. GPC was used as an independent, conventional cross-check on the comonomer conversion provided by the numerical approach to the PDA data outlined below. The detector train included a home-built viscometer, a Brookhaven Instruments Corporation BIMwA light scattering detector, and Shimadzu RID-10A refractive index and SPD-10AVvp ultraviolet/vis detectors. The GPC eluent, butyl acetate, was passed through detectors and columns using an LC-ATvp Shimadzu HPLC pump.

The two GPC columns were a gift from Polymer Laboratories Inc. and comprised PLgel 5 μm 500 Å, 300 × 7.5 mm in series with PLgel 5 μm 50 Å, 300 × 7.5 mm. The injector loop was 100 μL and a flow rate of 1 mL/min was used.

Unless stated otherwise, all the injected solutions were aliquots from ACOMP reactions (waste line) diluted 1:10 and filtered with 0.45 μm PTFE syringe filters. UV chromatograms at 254 nm were used in computing fractional comonomer conversion by integrating the peaks obtained by separation of the species eluted.

The UV peaks were integrated to obtain the concentration of each comonomer for each elution profile. Figure 1 is representative of the GPC data from aliquots withdrawn at different times from the reactor. The first peak at about 1180 s is due to BA; the second at 1260 s is due to MMA.

Full Spectrum Approach to Comonomer Conversion. In principle, it suffices at any instant to have two distinct signals consisting of contributions from comonomers A and B in order to exactly solve for each comonomer concentration at that instant. This was used, for example, in previous ACOMP work to separate styrene and methyl methacrylate concentrations by using an RI signal and a single UV wavelength, where each comonomer contributed very differently to each of the two signals. When the contributions to the signals from each comonomer are similar, however, the "exact" solution of the two simultaneous equations becomes dominated by noise, and the procedure is no longer reliable. It is also necessary to know whether and how much the copolymer being synthesized itself contributes to the signal at each point in the spectrum.

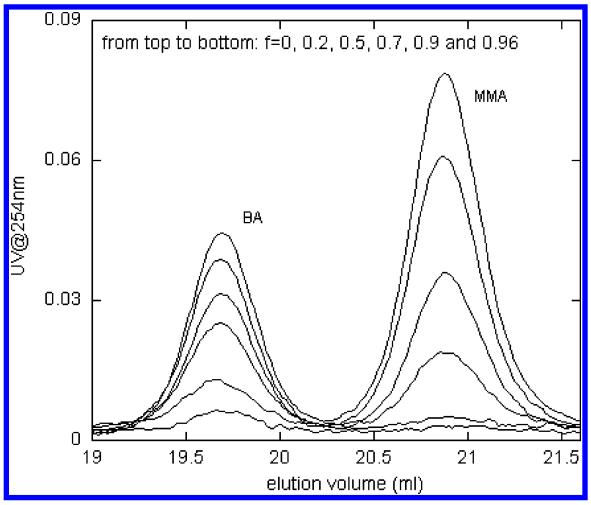

Figure 1. Raw GPC chromatograms showing the reduction of the MMA and BA monomer UV signals at different points of conversion for experiment #3 in Table 1. The first peak at 19.8 mL corresponds to BA, and the second at 21 mL to MMA. The residual BA at high conversion is also seen.

The working hypothesis in this presentation is that, if many signals from a spectrum are used, each of which has a small, but distinct difference in the contribution from comonomers A and B, then the precision of the comonomer concentration determination can be increased dramatically over two signal approaches. The degree to which this is true depends on the detailed difference in spectra between A and B. The approach is general, in that it will apply for absorption and emission spectra in any wavelength region of the electromagnetic spectrum, including IR, where there are small but measurable differences between the spectra of A and B.

The only assumption in this approach is that the spectrum obtained from a highly dilute, quenched sample of the reacting solution at any instant is a linear superposition of spectral contributions from comonomers A and B and the copolymer itself. This condition will always be met in dilute solutions as long as the comonomers and/or copolymer do not interact to form some concentration-dependent associated species whose spectrum is different than simply the sum of component spectra. There are no assumptions about the shape of peaks or the locations of their maxima nor any modeling or fitting routines involved in this approach.

Let $S(\lambda)$ be an absorbance (or emission) signal at wavelength λ given by

$$S(\lambda) = \epsilon(\lambda)cL \tag{1}$$

where L is the sample cell path length in cm, and for experimental convenience c is the solute concentration in g/cm^3, so that $\epsilon(\lambda)$ is the mass concentration extinction coefficient (cm^2/g). Let $\epsilon_i(\lambda)$ and c_i be the extinction coefficient and mass concentration, respectively, of comonomer i at wavelength λ. Then $S(\lambda)$ is given by

$$S(\lambda) = L\sum_{i=1}^{N}[\epsilon_i(\lambda)c_i + \epsilon_{p,i}(\lambda)c_{p,i}] + L\sum_{m=1}^{M}\epsilon_m(\lambda)c_m \tag{2}$$

where N is the number of comonomers and the sum includes signal due to all the comonomers and the copolymers, where $c_{p,i}$ represents

the concentration of comonomer i in copolymeric form, and $\epsilon_{p,i}(\lambda)$ is the extinction coefficient of the polymeric form of comonomer i. The appearance of the $c_{p,i}$ terms does not increase the number of unknowns, which continues to be the N comonomer concentrations, since mass balance requires

$$c_{p,i} = c_{i,0} - c_i \tag{3}$$

where $c_{i,0}$ is the initial concentration of c_i. (In this work 70% of the reactor liquid is solvent, so density changes are ignored. Density corrections have been used in refs 41 and 45.) The right-hand term is a sum over M possible other signal producing species, such as the initiator. An important case of this in future work may be where the ACOMP dilution solvent is different from the solvent in the reactor. In this work, since the initiator had no significant absorption at the low concentrations used, and the reactor and dilution solvent were the same, the right-hand term was not important.

The time-dependent concentration of each comonomer i, $c_i(t)$, is found at each point in time by minimizing the mean square error, $M(t)$, where

$$\mathrm{M}(t) = \frac{\sum_j w(\lambda_j)\{S_{exp}(\lambda_j,t) - S_{calc}(\lambda_j,t)\}^2}{\sum_j w(\lambda_j)} \tag{4}$$

where $S_{exp}(\lambda_j,t)$ is the signal measured by ACOMP and $S_{calc}(\lambda_j,t)$ is the absorbance value calculated according to eq 2. The sum in j is over all wavelengths in the range of interest. $w(\lambda_j)$ is a weighting factor, which, in this work is chosen to be unity for all λ_j, since that preferentially weights the larger signals, rather than choosing $w(\lambda_j)$ to be inversely proportional to the signal, or the signal squared, as is sometimes done to give each term a fractional representation.

$M(t)$ can be separately minimized with respect to each independent component by partial differentiation, and solving the resulting set of linear equations by standard matrix methods, yielding the concentrations of the comonomers at each instant t. Online knowledge of the comonomer concentration functions gives extraordinary power to follow composition drift and hence the evolution of the composition distribution, and they are also used to determine the time course of the average molar mass and intrinsic viscosity distributions.

Minimization of $M(t)$ yields the matrix equation

$$\bar{A} = \bar{c} \bullet \bar{\bar{B}} \tag{5}$$

where the elements of vector $\bar{A}$ are given by

$$A_n = \sum_j \delta_n(\lambda_j) w(\lambda_j)[S_{exp}(\lambda_j) - L\sum_i \epsilon_{p,i}(\lambda_j) c_{i,0}] \tag{6}$$

The elements of vector $\bar{c}$ are simply the comonomer concentrations c_k and $\bar{\bar{B}}$ is a square, symmetric matrix of dimension N, where N is the total number of comonomers, whose elements are given by

$$B_{k,n} = L\sum_j \delta_k(\lambda_j)\delta_n(\lambda_j) w(\lambda_j) \tag{7}$$

where

$$\delta_k(\lambda_j) = \epsilon_k(\lambda_j) - \epsilon_{p,k}(\lambda_j) \tag{8}$$

Explicitly inverting $\bar{\bar{B}}$ and solving for $\bar{c}$ for the case where $N = 2$, appropriate to this work, yields

$$c_1(t) = \frac{A_1(t)B_{22}(t) - A_2(t)B_{12}(t)}{B_{11}(t)B_{22}(t) - B_{12}(t)^2} \tag{9}$$

where the symmetry of $\bar{\bar{B}}$ has been used to take $B_{12}(t) = B_{21}(t)$. c_2 is found by interchanging indices 1 and 2 in eq 9.

Alternatively, microcomputers are speedy enough to do rapid, fine searches in parameter space to locate the minimum of $M(t)$. This latter, computationally more intensive approach was used to cross-check the code developed for the matrix approach.

Error Analysis. Computation of $c_1(t)$ and $c_2(t)$ according to the above procedure produces the values of minimum error at each instant. It is convenient to assess the error in terms of the net fractional error at each point in time, defined by

$$\mathrm{E}(t) = \frac{\sqrt{M(t)}}{\sum_j S_{exp}(\lambda_j,t)} \tag{10}$$

The steepness of $E(t)$ around the minimum is given in terms of the partial derivatives

$$\mathrm{d}E(t,c_1,\ldots c_N) = \sum_k \frac{\partial E}{\partial c_k}\mathrm{d}c_k \tag{11}$$

where the derivative for the concentration of monomer k, c_k, is

$$\frac{\partial E}{\partial c_k} = \frac{\sum_j w(\lambda_j)\{|S_{exp}(\lambda_j,t) - S_{calc}(\lambda_j,t)|(\epsilon_k(\lambda_j) - \epsilon_{p,k}(\lambda_j))\}}{\sum_j w(\lambda_j) S_{exp}(\lambda_j,t)\sqrt{M(t)}} \tag{12}$$

The larger the derivative, the steeper the walls of the "error valley" and hence the more accurate the values of c_k at the bottom of the valley are.

Results

Typical Raw ACOMP Data. Table 1 lists the conditions of the five copolymerization experiments monitored by ACOMP. Table 2 gives relevant properties of the comonomers and the solvent. The values of dn/dc were computed from the ACOMP data according to the method of Brousseau et al.[49] The values for the comonomers in the table are averages over the five copolymerization experiments.

The raw RI and 90° LS data in Figure 2, from experiment no. 3, show typical behavior. The first 3000 s is the butyl acetate solvent baseline. BA was added at 3000 s and then MMA at 5000 s. The polymerization effectively begins at 7500 s, within a couple hundred seconds of adding the AIBN (the delay from reactor to detectors is about 180 s). The dn/dc of the comonomers in copolymeric form is significantly higher than in monomeric form (Table 2), so that RI increases strongly during the copolymerization reaction. Likewise, as more polymer is produced, the LS increases.

The raw ACOMP data for viscosity and one of the two UV wavelengths on the dual wavelength Shimadzu are shown (254 nm). UV absorption increases markedly with the addition of each monomer, whereas the viscometer does not sense the dilute monomer solution. Once the reaction begins, the UV decreases as the comonomers are consumed and lose their double bonds, whereas the viscosity increases with increasing concentration of polymer.

Extinction Coefficient Spectra. The analysis program developed computes the extinction coefficient basis spectra for the comonomers and the copolymer from the raw full UV spectrum ACOMP data. While the copolymer extinction coefficient basis spectra can be measured by precipitating copolymer from reactor aliquots, drying, redissolving, and measuring the spectra, a different, more efficient approach was taken here.

Table 1. Summary of Reactions, ACOMP Rate Constants, and ACM Values for End Product $[\eta]_w$, M_w, and A_2[a]

expt[b]	$C_{MMA,0}$ (g/cm^3)	$C_{BA,0}$ (g/cm^3)	a_{MMA} (s^{-1})	a_{BA} (s^{-1})	A_2 (cm^3/g^2 × M)	M_w (g/M)	$[\eta]_w$ (cm^3/g)
1. BA/MMA 10/90	250.6×10^{-3}	27.31×10^{-3}	2.46×10^{-4}	2.24×10^{-4}	3.47×10^{-4}	13 500	7.83
2. BA/MMA 25/75	206.1×10^{-3}	67.73×10^{-3}	3.29×10^{-4}	1.40×10^{-4}	6.09×10^{-4}	16 700	9.86
3. BA/MMA 40/60	163.6×10^{-3}	103.4×10^{-3}	2.88×10^{-4}	1.56×10^{-4}	7.67×10^{-4}	17 000	11.2
4. BA/MMA 50/50	138.8×10^{-3}	136.5×10^{-3}	4.00×10^{-4}	1.45×10^{-4}	7.90×10^{-4}	18 100	11.2
5. BA/MMA 75/25	67.3×10^{-3}	202.5×10^{-3}	7.29×10^{-4}	3.02×10^{-4}	11.0×10^{-4}	29 100	14.7

[a] AIBN 2% of total mass (wt %) was used as initiator for all the experiments. [b] Ratios are gram/gram.

Table 2. Summary of Properties of Comonomers and Corresponding Homopolymers

	MMA	BA	PMMA	PBA	BAc
d*n*/d*c*	0.0198	0.0278	0.0975[a]	0.0840[b]	NA
density (g/mL) at25C	0.936	0.894	NA	NA	0.881

[a] The d*n*/d*c* values for comonomers are averages of d*n*/d*c*'s computed in the experiments listed in table above. [b] The d*n*/d*c* values for homopolymers are averages of d*n*/d*c*'s computed in different experiments.

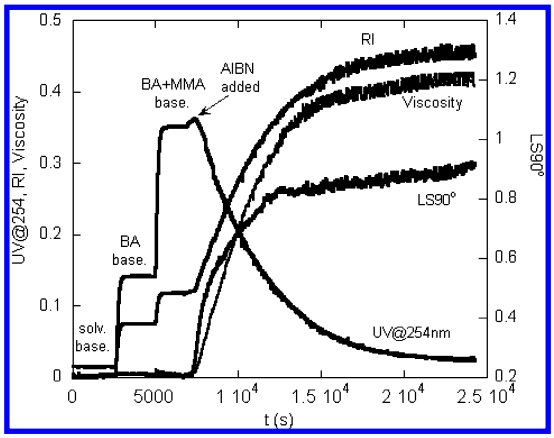

Figure 2. Raw LS, RI, UV (at 266 nm), and viscosity data for the BA/MMA (40/60, g/g) copolymerization.

Namely, the ACOMP reaction spectra themselves were used to determine $\epsilon_p(\lambda_j)$ in the following way: By setting $\epsilon_p(\lambda_j) = 0$ in a first pass on the data analysis over a range where the polymer has no significant absorption (250−290 nm was used), the systematic, residual difference between the experimental spectrum at each time point and the optimized comonomer spectrum is the copolymer spectrum. Since the concentration of each comonomer is known from the minimization procedure, the copolymer concentration is also known, and hence $\epsilon_p(\lambda_j)$ can be computed. Since this procedure can be carried out at every point in time it is also possible to monitor how $\epsilon_p(\lambda_j)$ changes as copolymer composition changes, so that $\epsilon_{p,i}(\lambda_j)$ for each comonomeric component can be computed. In this work, however, it was found that all $\epsilon_p(\lambda_j)$ are very small compared to the comonomer $\epsilon(\lambda_j)$ and no significant change was found for different compositions of BA/MMA.

Figure 3 gives extinction coefficient basis spectra, averaged over the five experiments. On the basis of the standard deviation from these, the variation from spectrum to spectrum for the five experiments was less than 5% over the wavelength range 235−300 nm. While this represents very good reproducibility and gives confidence in using standard extinction coefficient basis spectra for monomers in given solvents, in this work the extinction coefficient spectrum determined in an experiment was the spectrum used for the analysis of that experiment. It was determined that the comonomer concentration results were not sensitive to selecting different ranges within the 235−300 nm band, although error bars changed. The range of 250−290 nm was selected for all final analyses.

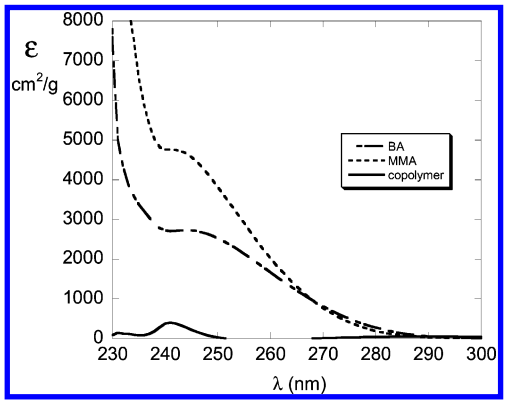

Figure 3. Average extinction coefficient basis spectra for MMA, BA and the copolymer.

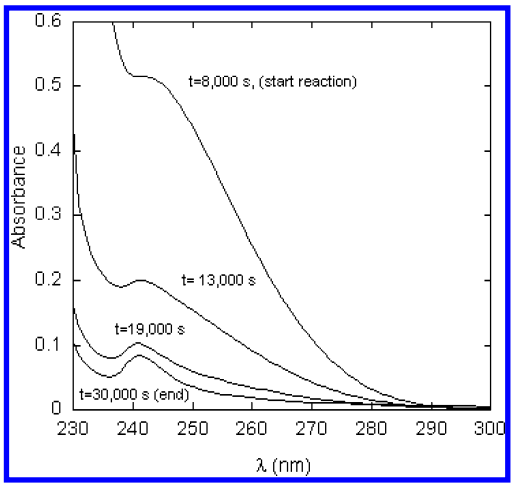

Figure 4. UV spectra from different times during the 50/50 copolymerization reaction. The times shown are from the time axis of Figures 2a,b.

The absorption of the polymer seen in Figure 3 is extremely small, but its contribution becomes important at high levels of conversion. Also, the polymer spectrum was computed at different degrees of conversion, and there is very little difference, showing the effects of composition drift, in this study, at any rate, are not important. That could change, of course, especially if one of the comonomers has a significant spectrum associated with a functional group. The evolution of the spectra at various points in the reaction is shown in Figure 4. The final spectrum contains both the copolymer contribution to the spectrum, and that of the residual BA.

Concentration Data with Fits. The analysis program uses the above error minimization procedure to extract the comonomer concentrations at each point from the raw ACOMP data. The extracted comonomer concentrations for experiment 3 are shown in Figure 5. In this figure $t = 0$ is the time the reaction began; i.e., the preceding baseline gathering time is subtracted from the raw data. The wavelength range from 250 to 290 nm at 1 nm intervals was used in the computation. Also shown are first order fits to the curves. The large, discrete points are results

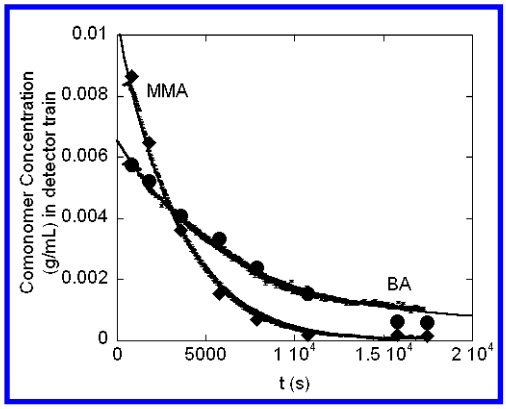

Figure 5. Comonomer concentrations vs time during the copolymerization reaction no. 3, using the error minimization procedure outlined in the text. The large, discrete points are independent GPC cross-checks on conversion from manually withdrawn reaction aliquots, using UV chromatograms, such as in Figure 1. The thickness of the lines is due to inclusion of error bars according to eq 12.

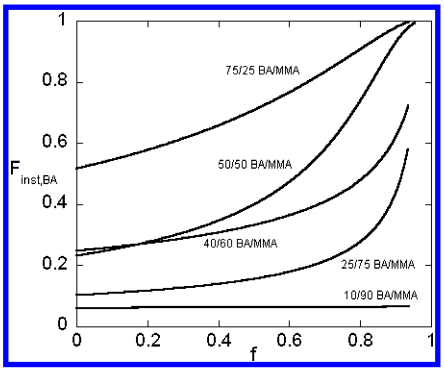

Figure 6. Composition drift for the copolymer reactions in Table 1.

from GPC on manually withdrawn reaction aliquots, using the methods described above. The agreement between the ACOMP and GPC data was excellent for all experiments. The error bars are also in place on the comonomer concentrations if Figure 5, seen in the width of the data lines, were computed according to eq 12, setting the error interval $\Delta E(t)$ equal to the actual minimum error at each point.

Composition Drift. The comonomer profiles can be used to compute the composition drift of the copolymer chains during synthesis. The average instantaneous fraction of BA by mass in a copolymer chain formed at any given moment is

$$F_{\text{inst,BA}} = \frac{\mathrm{d}c_{\text{BA}}}{\mathrm{d}(c_{\text{BA}} + c_{\text{MMA}})} \tag{13}$$

Figure 6 is derived from the exponential fits above and the equation for $F_{\text{inst,BA}}$. It is plotted vs f_{total}, the total fractional mass conversion of comonomers, given by

$$f_{\text{total}} = \frac{c_{\text{p,MMA}} + c_{\text{p,BA}}}{c_{\text{BA,0}} + c_{\text{MMA,0}}} \tag{14}$$

Figure 6 shows how strongly the composition drifts due to the large difference in conversion rates of BA and MMA. Because MMA converts more quickly than BA, higher percentages of BA in the starting solution lead to larger composition drifts toward high fractions of BA, as the MMA is depleted earlier in the reaction. None of the starting compositions led to an azeotropic condition, although 10/90 g/g/ of BA/MMA comes very close.

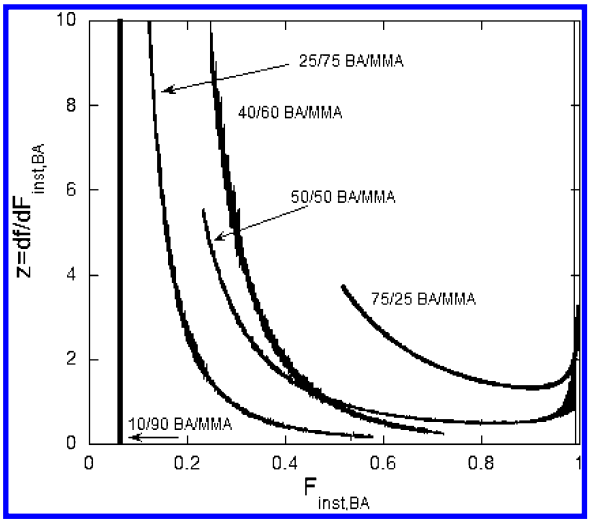

Figure 7. Average composition distributions for the copolymer reactions in Table 1.

Average Composition Distribution. The average composition distribution can be computed from the above data according to

$$z = \mathrm{d}(f_{\text{total}})/\mathrm{d}F_{\text{inst,BA}} \tag{15}$$

where $z\mathrm{d}F_{\text{inst,BA}}$ is the fraction of the total population of chains with mass composition of BA between $F_{\text{inst,BA}}$ and $F_{\text{inst,BA}} + \mathrm{d}F_{\text{inst,BA}}$. The computation of z is shown in Figure 7. As expected, the copolymer with highest starting MMA/BA ratio has both the highest drift and broadest composition distribution. The case of lowest BA/MMA (10/90) has very little composition drift, and the distribution is essentially a delta function, as represented by the vertical line in Figure 7.

ACOMP does not furnish the instantaneous width of the composition distribution, rather the average value, hence the term "average composition distribution". In ref 42 the average composition distribution was folded with the Stockmayer distribution to visualize the full composition distribution.

Reactivity Ratios. Although in some sense ACOMP obviates the need for reactivity ratios, in that the average composition drift and distribution are monitored directly throughout the reaction, the reactivity ratios still are important for their predictive power, their practical use in helping to optimize reactions, their inherent theoretical interest, and for historical reasons.

The usual Mayo-Lewis copolymer equation is

$$\frac{\mathrm{d[A]}}{\mathrm{d[B]}} = \frac{[\mathrm{A}]}{[\mathrm{B}]}\left(\frac{r_{\text{A}}[\mathrm{A}] + [\mathrm{B}]}{[\mathrm{A}] + r_{\text{B}}[\mathrm{B}]}\right) \tag{16}$$

where r_{A} and r_{B} are the reactivity ratios of comonomers A and B, and [A], [B] are the molar concentration of comonomers A and B, respectively, in contrast to their mass concentrations (g/cm^3), represented as c_{A} and c_{B}, throughout this work. Interestingly, the comonomer conversion curves in this work are all very well approximated by exponential fits of the form

$$[\mathrm{A}](t) = [\mathrm{A}]_0 \exp(-\alpha_{\text{A}} t) \tag{17a}$$

$$[\mathrm{B}](t) = [\mathrm{B}]_0 \exp(-\alpha_{\text{B}} t) \tag{17b}$$

Table 3. Compilation of Reactivity Ratios: This Work and Literature

r_{BA}	r_{MMA}	conditions	source
0.40 ± 0.05	2.58 ± 0.6		averages, this work
0.36	2.55		Buback et al.[67]
0.349	2.06	benzene	Madruga and Fenandez-Garcia[60]
0.395	2.28	toluene	Aerts et al.[68]
0.253	1.550	benzonitrile, 50 °C	De la Fuente and Madruga[69]
0.298	1.789	bulk	Dubé and Penlidis[70]
0.357	2.51	bulk 50 °C	Hutchinson et al.[71]
0.37	1.8	60 °C	Grassie et al.[72]
0.47	2.56	60 °C	Han and Wu (in ref 71)
0.46	2.4	100 °C	Han and Wu (in ref 71)
0.32	1.94	toluene 60 °C	Hakim et al.[73]
0.31	1.88	toluene 80 °C	Hakim et al.
0.36	2.07	ATRP, ethyl acetate 90 °C	Roos et al.[74]
0.37	3.15	ATRP, bulk, 90 °C	Ziegler and Matyjaszewski[75]
0.27	2.52	ATRP, bulk, 90 °C	Ziegler and Matyjaszewski
0.36 ± 0.06	2.29 ± 0.4	$\langle r_{BA}\rangle\langle r_{MMA}\rangle = 0.82$	

When this is the case, then the Mayo Lewis equation becomes

$$\frac{\alpha_A}{\alpha_B} = \frac{r_A[A](t) + [B](t)}{[A](t) + r_B[B](t)} \tag{18}$$

It is straightforward to prove that in this case, the only way this equation can hold is if

$$r_A = \frac{\alpha_A}{\alpha_B}, \quad r_B = \frac{\alpha_B}{\alpha_A} \tag{19}$$

And so it is also true that $r_A r_B = 1$.

The instantaneous mole fraction of monomer A, [A], incorporated, $F_{A,inst}$, is given by

$$F_{A,inst} \equiv \frac{d[A]}{d[A+B]} = \frac{r_A f_A^2 + f_A(1-f_A)}{r_A f_A^2 + 2f_A(1-f_A) + r_B(1-f_A)^2} \tag{20}$$

where f_A and f_B are the mole fractions of monomer A and B, respectively, at any instant

$$f_A = \frac{[A]}{[A]+[B]}, \quad f_B = \frac{[B]}{[A]+[B]} \tag{21}$$

$F_{B,inst}$ is obtained by interchanging the subscripts A and B. These expressions form the basis for finding composition as a function of conversion, and determining sequence length distributions. These topics are not pursued here.

The histograms in parts a and b of Figure 8 show the distribution of reactivity ratios from the literature, numerical values of which are given in Table 3 below. Although reactivity ratios were measured for MMA/BA under a wide variety of conditions—varying temperatures, solvent, and polymerization mode (e.g., free radical vs ATRP)—the values are fairly well clustered, as seen in the histograms, and in the error bars on the reactivity ratios.

The current results are well within the range of reported values, adding confidence to the ACOMP method as it is used to study an increasing range of copolymerization reactions.

Molar Mass and Intrinsic Viscosity. The reduced viscosity η_r, and M_w data indicate small polymers are produced. Figure 9 shows the evolution of M_w and weight-average intrinsic viscosity $[\eta]_w$ during a typical copolymerization reaction, no. 3 in Table 1. Given the low value of reduced viscosity, and the low concentration of polymer in the detector train $[\eta]_w$ is taken equal to η_r.

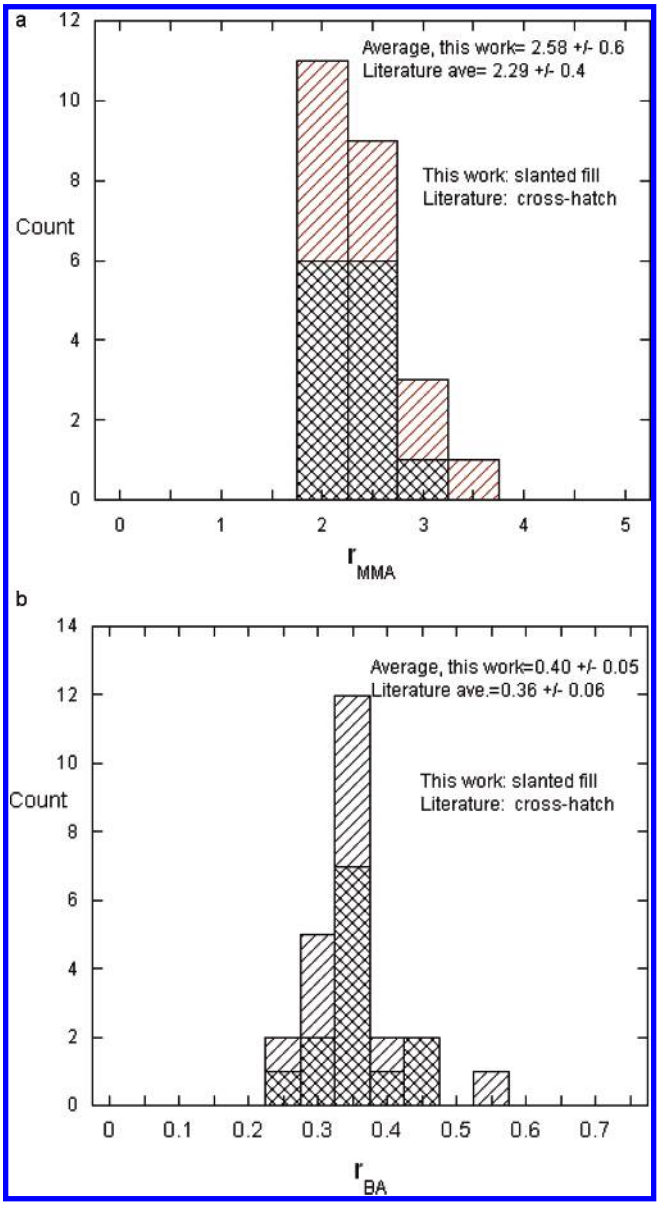

Figure 8. (a) Histogram of literature values and those from this work for the MMA reactivity ratio r_{MMA}. (b) Histogram of literature values and those from this work for the BA reactivity ratio r_{BA}.

It is noted that determination of copolymeric M_w from light scattering is considerably more involved than homopolymeric

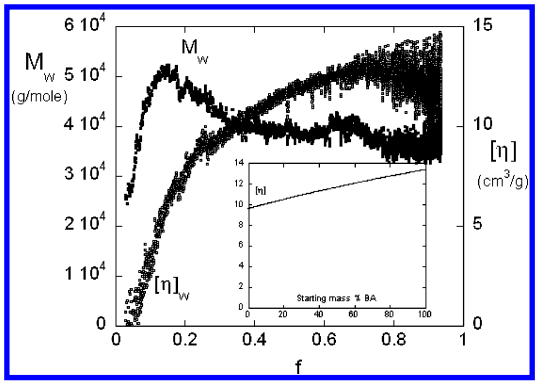

Figure 9. Evolution of M_w and $[\eta]_w$ during reaction no. 3. The inset shows the persistence length based computation of $[\eta]_w$ for a copolymer of fixed $M_w = 20\,000$ g/mol, whose starting mass fraction of BA varies from 0% to 100%.

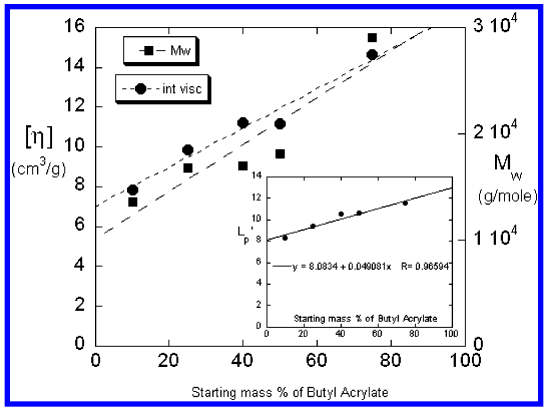

Figure 10. ACM results for the endproducts of the five copolymer reactions in Table 1. The stiffening effect of BA on the chain is shown via the viscosity-derived apparent persistence length L_p', shown in the inset vs starting percentage of BA.

M_w determination. The original analyses of this problem were carried out by Bushuk and Benoit[50] and Stockmayer et al.,[51] who demonstrated that the mass obtained by the homopolymeric approach is only an apparent mass $M_{w,ap}$, which is related via the composition distribution and the dn/dc of the respective comonomers in polymeric form to the true M_w. The several anomalies that can appear in light scattering data from copolymeric solution have been noted from time to time in the literature.[52,53] It was recently demonstrated that ACOMP can avoid the traditional difficulties of finding M_w from copolymers, because the instantaneous and cumulative compositions of the copolymer are known at every moment during the copolymerization reactions.[42] In the case at hand, the differences in dn/dc for MMA and BA are so small (see Table 2) that the difference between $M_{w,ap}$ and M_w is less than 3%, even when considerable composition drift occurs.

Figure 10 shows the final values of M_w and $[\eta]_w$ from ACOMP for all the reactions vs the starting mass percentage of BA. Linear fits to each are shown as guides to the eye, since there is no reason to expect a linear relationship as a function of this variable. The copolymers are too small to measure an angular dependence in light scattering and hence the z-average mean square radius of gyration $\langle S^2\rangle_z$ cannot be measured. $[\eta]_w$ is used, instead, to obtain the root-mean-square viscometric radius of gyration given (for ideal coils) by

$$\langle S^2\rangle_V^{1/2} = \frac{1}{\sqrt{6}}\left(\frac{M[\eta]}{\Phi}\right)^{1/3} \tag{22}$$

From this the *apparent* persistence length[54−56] L_p', is found in the coil limit of the wormlike chain formula

$$L_p' = \frac{3\langle S^2\rangle}{L} \tag{23}$$

where the average contour length L, is estimated via

$$L(\text{Å}) = \frac{M}{\left(\frac{[\text{pMMA}]_f\, m_{MMA} + [\text{pBA}]_f\, m_{BA}}{2.56([\text{pMMA}]_i + [\text{pBA}]_i)}\right)} \tag{24}$$

$[\text{pMMA}]_i$ and $[\text{pBA}]_i$ are the initial molar concentrations of pMMA and pBA, respectively, and m_{MMA} and m_{BA} are the monomer molar masses. The inset to Figure 10 shows L_p' as a function of initial composition. There is a significant increase in L_p' as BA composition increases, meaning that chains with high BA content are stiffer than those with high MMA content. This is consistent with the fact that BA has a much larger functional group, and hence more steric hindrance, than MMA. It also indicates that the steric effect of the pendant group in the acrylate (BA) in determining chain stiffness overshadows the effect of the methyl group in the methacrylate (MMA).

L_p' for pure pMMA from a literature report[57] gives 8.1 ± 0.5 Å, in agreement with the inset's intercept of 8.1 Å. Data from ref 45 yields $L_p' = 13.1 \pm 1.1$ Å for pure pBA, in agreement with the inset's intercept of 13.0 Å.

Further evidence of the stiffening effect of BA on the copolymer is seen in Table 1, where A_2 increases strongly with the fractional content of BA. A_2 is related to the RMS radius of gyration via

$$A_2 = \frac{16\pi N_A(a\langle S^2\rangle^{1/2})^3}{3M^2} \tag{25}$$

where a is a dimensionless constant, normally smaller than 1. Taking the viscosity derived radius of gyration as the one in eq 25, yields an average value $a = 0.76 \pm 14\%$, using the ACM values of $[\eta]_w$ and A_2 in Table 1.

The inset to Figure 9 shows how $[\eta]_w$ is computed to change as the starting composition of BA changes, for a fixed $M_w = 20\,000$. This may partly explain the countervailing trends of increasing $[\eta]_w$ while decreasing M_w vs f for a portion of the conversion. There may be other effects involved, but GPC results, for example, show that polydispersity during the reactions does not change significantly (data not shown). Otherwise the countervailing trend may have indicated decreasing polydispersity, which is not the case.

Although it is beyond the scope of the current work to find a definitive explanation, the unusual evolution of M_w and $[\eta]_w$ may be related to several possible effects: (1) The large disparity in the MMA/BA reactivity ratios, (2) branching, and (3) a variety of solvent based effects.[58] It has often been found that alkyl acrylates, such as BA, have polymerization rates, d[BA]/dt that are proportional to $[\text{BA}]^d$, where d ranges from 1.4 to 1.8, instead of $d = 1$.[59−62] Explanations include chain length dependence of termination rate coefficients,[63] monomer/solvent complexation,[64] and intrachain radical transfer to form a propagating, midchain radical, leading to a form of branching.[65,66] Presumably, there could be a corresponding interchain end to midchain transfer as well, that could lead to reinitiation and increased M_w of "dead" chains. Since ACOMP furnishes kinetics, M_w and $[\eta]_w$ without any model dependent assumptions, any such effects mentioned above are implicitly included in the

ACOMP results. ACOMP is hence promising for addressing some of the many effects described in the literature.

Conclusions

This work presents a means of following the evolution of average composition, molar mass, and intrinsic viscosity distributions during the copolymerization of comonomers with similar spectral characteristics. The separation of instantaneous comonomer concentrations was achieved using full spectrum data, in this case UV absorption, analyzed by an error minimization procedure that required no a priori model assumptions.

The ACOMP method was applied to the case of BA/MMA copolymerization with different starting compositions. The conversion results from the full spectrum ACOMP approach were cross-checked by GPC using UV detection, and the agreement was excellent in each case. A wide variation in composition drift and distribution was found, the drift and width of the distributions becoming wider as the amount of BA is increased. No starting mixture yielded an azeotropic condition, although the BA/MMA 10/90 g/g came very close. M_w and $[\eta]_w$ decrease as the starting ratio of MMA/BA increases. Reactivity ratios were computed and the values are well within the error bars of results tabulated from many literature sources.

This work sets the stage for online control of copolymerization, including CRP and other "living" mechanisms, for optimizing reactions, providing data to assess kinetic theories of copolymerization, and for extension to terpolymerization. The robustness of the method is currently under further investigation, as well as its extension to infrared detectors.

Acknowledgment. The authors acknowledge support from Arkema Inc., NSF CTS 0623531, NASA NCC3-946, and the Louisiana Board of Regents LINK program and ITRS RD-B-07. All the authors were displaced from New Orleans in August 2005, due to Hurricane Katrina. They would like to thank Professors David Hoagland, Shaw Ling Hsu, Thomas Russell, and other members of the Polymer Science & Engineering Department at the University of Massachusetts at Amherst for the warm welcome extended to them in Katrina's aftermath. Much of the current work was carried out at the University of Massachusetts, and support from the NSF-funded MRSEC is also acknowledged. The authors further thank the following entities for generous help in terms of instrument loans and donations used to set up an ACOMP system at the University of Massachusetts: Polymer Laboratories Inc., Brookhaven Instruments Corp., and Shimadzu Corp.

References and Notes

(1) Hadjichristidis, N.; Pispas, S.; Floudas, G. *Block copolymers; synthetic strategies, physical properties and applications*; John Wiley & Sons: New York, 2003.
(2) Rodriguez, F. *Principles of Polymer Systems*, 3rd ed.; Hemisphere Publishing: Bristol, PA, 1989.
(3) Odian, G. *Principles of Polymerization*, 3rd eds.; John Wiley & Sons: New York, 1991.
(4) Stepanek, P.; Lodge, T. P. In *Light Scattering, Principles and Development*; Brown, W., Ed.; Oxford Sci. Pub.: Oxford, U.K., 1996.
(5) Hanley, K. J.; Lodge, T. P.; Huang, C. I. *Macromolecules* **2000**, *33*, 5918.
(6) Pitsikalis, M.; Siadali-Kioulafa, E.;N. Hadjichristidis, N. *Macromolecules* **2000**, *33*, 5460.
(7) Chitanu, B. C.; Skouri, M.; Schosseler, F.; Munch, J. P.; Carpov, A.; Candau, S. J. *Polymer* **2000**, *41*, 3638.
(8) Kim, C.; Lee, S. C.; Shin, J. J.; Yoon, J. S.; Kwon, I. C.; Jeong, S. Y. *Macromolecules* **2000**, *33*, 7448.
(9) Seo, Y.; Esker, A. R.; Sohn, D.; Kim, H.-J.; Park, S.; Yu, H. *Langmuir* **2003**, *19*, 3313.
(10) Kim C.; Yu, H. *Langmuir* **2003**, *19*, 4460.
(11) Ghosh, K.; Carri, G. A.; Muthukumar, M. *J. Chem. Phys.* **2002**, *116*, 5299.
(12) Stockmayer, W. H. *J. Chem. Phys.* **1945**, *13*, 199.
(13) Tobita, H. *Polymer* **1998**, *39*, 2367.
(14) Shaw, B. M.; McAuley, K. B.; D. W. Bacon, D. W. *Polym. React. Eng.* **1998**, *6*, 113.
(15) Mayo, F. R.; Lewis, F. M. *J. Am. Chem. Soc.* **1944**, *66*, 1594.
(16) Shaikh, S.; Puskas, J. E.; Kaszas, G. *J. Polym. Sci., A: Polym. Chem.* **2004**, *42*, 4084.
(17) Dube, M.; Sanayei, R. A.; Penlidis, A.; Driscoll, K. F.; Reilly, P. M. *J. Polym. Sci., Part A: Polym. Chem.* **1991**, *29*, 703.
(18) McKenna, T. F.; Fevotte, G.; Graillat, C.; Guillot, J. *Chem. Eng. Res., Des*, **1996**, *74* (A3), 340.
(19) Sauzedde, F.; Hunkeler, D. *Int. J. Polym. Anal. Charact.* **2001**, *6*, 295.
(20) Wild, L. *Adv. Polym. Sci.* **1991**, *98*, 1.
(21) Anantawaraskul, S.; Soares, J. B. P.; Wood-Adams, P. *J. Polym. Sci., B: Polym. Phys.* **2003**, *41*, 1762.
(22) Feng, Y.; Hay, J. N. *Polymer* **1998**, *39*, 6723.
(23) Zacur, R.; Goizueta, G.; Capiati, N. *Polym. Sci. Eng.* **2000**, *40*, 1921.
(24) Anantawaraskul, S.; Soares, J.; Wood-Adams, P. M. *Macromol. Chem. Phys.* **2004**, *205*, 771.
(25) Meehan, E.; O'Donohue, S. *Adv. Chem. Ser.* **1995**, *247*, 243.
(26) Netopilik, M.; Bohdanecky, M.; Kratochvil, P. *Macromolecules* **1996**, *29*, 6023.
(27) Kramer, I.; Pasch, H.; Handel, H.; Albert, K. *Macromol. Chem. Phys.* **1999**, *200*, 1734.
(28) Montaudo, M. S. *NMR Spectroscopy of Polymers in Solution and in the Solid State*; ACS Symposium Series 834; American Chemical Society: Washington, DC, 2003.
(29) Tacx, J. C. J. F.; German, A. L. *Polymer* **1989**, *30*, 918.
(30) Mori, S. *Anal. Chem.* **1988**, *60*, 1125.
(31) Philipsen, J. A. H. *J. Chromatogr.* **2004**, *1037*, 329.
(32) Chang, T. *J. Polym. Sci., Part B: Polym. Phys.* **2005**, *43*, 1591.
(33) Reis, M. M.; Araujo, P. H. H.; Sayer, C.; Giudici, R. *Macromol. Symp.* **2004**, 206; Polym. React. Eng. **2004**, *5*, 165.
(34) Van den Brink, M.; Pepers, M.; Van Herk, A. M.; German, A. L. *Polym. React. Eng.* **2001**, *9*, 101.
(35) Wang, C.; Vickers, T. J.; Schlenoff, J. B.; Mann, C. K. *Appl. Spectrosc.* **1992**, *46*, 1729.
(36) Shaikh, S.; Puskas, J. E. *Polym. News* **2003**, *28*, 71.
(37) Long, T. E.; Liu, H. Y.; Schell, B. A.; Teegarden, D. M.; Uerz, D. S. *Macromolecules* **1993**, *26*, 6237.
(38) Vieira, R.; Sayer, C.; Lima, E.; Pinto, J. *J. Appl. Polym. Sci.* **2002**, *84*, 2670.
(39) Fontoura, J. M. R.; Santos, A. F.; Silva, F. M.; Lenzi, M. K.; Lima, E. L.; Pinto, J. C. *J. Appl. Polym. Sci.* **2003**, *90*, 1273.
(40) Florenzano, F. H.; Strelitzki, R.; Reed, W. F. *Macromolecules* **1998**, *31*, 7226.
(41) Mignard, E.; Leblanc, T.; Bertin, D.; Guerret, O.; Reed, W. F. *Macromolecules* **2004**, *37*, 966.
(42) Catalgil-Giz, H.; Giz, A.; Alb, A. M.; Oncul, A. K.; Reed, W. F. *Macromolecules* **2002**, *35*, 6557.
(43) Elizalde, O.; Asua, J. M.; Leiza, J. R. *Appl. Spectrosc.* **2005**, *59*, 1280.
(44) Reis, M. M.; Araujo, P. H. H.; Sayer, C.; Giudici, R. *J. Appl. Polym. Sci.* **2004**, *93*, 1136.
(45) Chauvin, F.; Alb, A.; Bertin, D.; Tordo, P.; Reed, W. F. *Macromol. Chem. Phys.* **2002**, *203*, 2029.
(46) Alb, A. M.; Farinato, R.; Calbeck, J.; Reed, W. F. *Langmuir* **2006**, *22*, 831.
(47) Norwood, D. P.; Reed, W. F. *Int. J. Polym. Anal. Charact.* **1997**, *4*, 99.
(48) Strelitzki, R.; Reed, W. F. *J. Appl. Polym. Sci.* **1999**, *73*, 2359.
(49) Brousseau, J.-L.; Giz, H.Ç.; Reed, W. F. *J. Appl. Polym. Sci.* **2000**, *77*, 3259.
(50) Bushuk, W.; Benoit, H. *Can. J. Chem.* **1958**, *36*, 1616.
(51) Stockmayer, W. H.; Moore, L. D.; Fixman, M.; Epstein, B. N. *J. Polym. Sci.* **1955**, *16*, 517.
(52) Tanaka, T.; Omoto, M.; Inagaki, H. *Macromolecules* **1979**, *12*, 146.
(53) Prud'homme, J.; Bywater, S. *Macromolecules* **1971**, *4*, 543.
(54) Reed, W. F. In *Macroion Characterization*"; Schmitz, K., Ed.; ACS Symposium Series 548; American Chemical Society: Washington, DC, 1994; pp 297−314.
(55) Reed, W. F.; Ghosh, S.; Medjahdi, G.; François, J. *Macromolecules* **1991**, *24*, 6189.
(56) Reed, C. E.; Reed, W. F. *J. Chem. Phys.* **1991**, *94*, 8479.
(57) Florenzano, F. H.; Fleming, V.; Enohnyaket, P.; Reed, W. F. *Eur. Polym. J.* **2005**, *41*, 535.
(58) Peck, A. N. F.; Hutchinson, R. A. *Macromolecules* **2004**, *37*, 5944.
(59) Scott, G. E.; Senogles, E. *J. Macromol. Sci. Chem.* **1970**, *A4*, 1105.
(60) Madruga, E. L.; Fernandez-Garcia, M. *Macromol. Chem. Phys.* **1996**, *197*, 3743.

(61) McKenna, T. F.; Villanueva, A.; Santos, A. M. *J. Polym. Sci., Part A: Polym. Chem.* **1999**, *37*, 571.
(62) Kaszas, G.; Foldes-Berezsnich, T.; Tudos, F. *Eur. Polym. J.* **1983**, *19*, 469.
(63) Fernandez-Garcia, M.; Fernandez-Sanz, M.; Madruga, E. L. *Macromol. Chem. Phys.* **2000**, *201*, 1840.
(64) Scott, G. E.; Senogles, E. *J. Macromol. Sci. Chem.* **1974**, *A8*, 753.
(65) Nikitin, A. N.; Hutchinson, R. A. *Macromolecules* **2005**, *38*, 1581.
(66) Nikitin, A. N.; Hutchinson, R. A. *Macromol. Theory Simul.* **2006**, *15*, 128.
(67) Buback, M.; Felderman, A.; Barner-Kowolik, C.; Lacik, I. *Macromolecules* **2001**, *34*, 5439.
(68) Aerts, A. M.; German, A. L.; van der Velden, G. P. M. *Magn. Reson. Chem.* **1994**, *32*, s80.
(69) De la Fuente, J.-L.; Madruga, E. L. *Macromol. Chem. Phys.* **1999**, *200*, 1639.
(70) Dubé, M. A.; Penlidis, A. *Polymer* **1995**, *36*, 587.
(71) Hutchinson, R. A.; McMinn, J. H.; Paquet, D. A.; Beuermann, S.; Jackson, C. *Ind. Eng. Chem. Res.* **1997**, *36*, 1103.
(72) Grassie, N.; Torrance, B. J. D.; Fortune, J. D.; Gemmell, J. D. *Polymer* **1965**, *6*, 653.
(73) Hakim, M.; Verhoeven, V.; McManus, N. T.; Dubé M. A.; Penlidis, A. *J. App. Polym. Sci.* **2000**, *77*, 602.
(74) Roos, S. G.; Mueller, A. H. E.; Matyjaszewski, K. *Macromolecules* **1999**, *32*, 8331.
(75) Ziegler, M. J.; Matyjaszewski, K. *Macromolecules* **2001**, *34*, 415−424.

MA060800F